

Direct Synthesis of Complex Loaded Chebyshev Filters in a Complex Filtering Network

Huan Meng, Ping Zhao, *Student Member, IEEE*, Ke-Li Wu, *Fellow, IEEE*,
and Giuseppe Macchiarella, *Fellow, IEEE*

Abstract—In this paper, a direct synthesis approach is proposed for designing a Chebyshev filter that matches the frequency variant complex loads at both the ports. The approach is based on the power wave renormalization theory and two practical assumptions: 1) the prescribed transmission zeros are stationary and 2) the reflection zeros are located along an imaginary axis. Three conditions are derived to stipulate the characteristic polynomials of the filter's responses through the renormalization of reference load impedances. These conditions are sequentially applied to ensure that the filter is physically realizable and well matched to the complex loads. It has been shown that the optimally synthesized filtering network that consists of an ideal filter cascaded with a piece of transmission line of an optimal length at each port can match the complex loads over a given frequency band with the best effort. By incorporating with an adjustment of the junction parameters, the approach provides an analytical yet flexible way to synthesize advanced microwave circuits composed of multiple filters connected together through some generalized junctions. The effectiveness of the method is demonstrated through three synthesis examples.

Index Terms—Dual multiplexer, filter combiner, filter synthesis, impedance matching, microwave filter.

I. INTRODUCTION

FILTER synthesis has been a classic research topic in the microwave engineering community over the past half century. Research efforts have been continuously devoted to the synthesis of microwave filters with required characteristics to satisfy the stringent channelization requirements in an increasingly sophisticated filtering network. A direct synthesis approach provides a circuit model for a physical filter design in a deterministic manner and is always preferred among various synthesis approaches.

A direct synthesis approach involves a sequence of analytical processes without any need for optimization. First, a set of characteristic polynomials defining a low-pass prototype filter is derived based on prescribed specifications. Then following a deterministic procedure, these characteristic polynomials are converted into a coupling matrix that produces exactly the same transferring and reflection responses. A series of

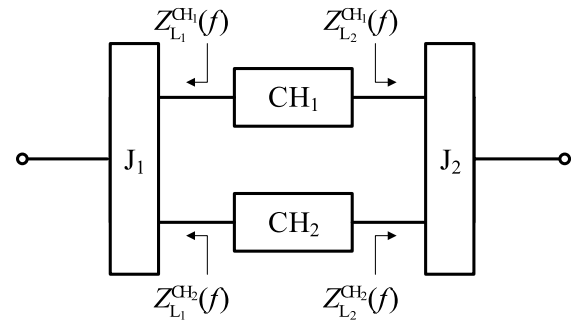


Fig. 1. Block diagram of a parallel-connected dual band filter.

similarity transforms are applied to reconfigure the coupling matrix to a desired topology to facilitate the physical realization. For the conventional direct synthesis approach [1], the conversion from characteristic polynomials into a coupling matrix presumes that the filter matches a real constant load at both the ports.

However, in practical applications, load impedances at a filter's port may not always be a real constant value. In some advanced microwave circuits, it is necessary to match a filter to a frequency varying complex load impedance at each port. Fig. 1 shows a block diagram of a parallel connected dual band filter [2] (also called a double-diplexed two-channel filter [3]) as an illustration. A parallel-connected dual band filter consists of two single bandpass filter connected in shunt between two junctions. Each filter therefore effectively becomes the loading for the other filter. Consequently, the load impedance Z_{L1}/Z_{L2} looking into the junction is a complex value and is a function of the physical frequency. Hence, the conventional synthesis theory cannot be directly applied. The design of filters in other advanced system, such as a masthead combiner [4] or in a dual multiplexer [5], also face the same problem. Unfortunately, to the author's best knowledge, such a practical synthesis problem has not been well addressed in the filter design community. A state-of-the-art design for such complex loaded filters relies on nonlinear optimization [5], [6]. The coupling matrices for each filter and the junction parameters are simultaneously optimized until the prescribed specifications are satisfied. However, as the number of channel filters grows, the number of optimization variables will rapidly increase and a brute-force optimization method becomes extremely time-consuming. Moreover, the optimization is susceptible to initial values and is easily trapped into local minimums, which may eventually fail to meet the design requirements. An investigation of optimization constraints for matching a filter to frequency variant loads was reported in [7].

Manuscript received June 28, 2016; revised September 22, 2016; accepted October 5, 2016. Date of publication October 28, 2016; date of current version December 7, 2016. An earlier version of this paper was presented at the 2016 International Microwave Conference, San Francisco, CA, USA, May 22–27, 2016.

H. Meng, P. Zhao, and K.-L. Wu are with the Department of Electronic Engineering, The Chinese University of Hong Kong, Hong Kong (e-mail: hmeng@ee.cuhk.edu.hk; pzao@ee.cuhk.edu.hk; kluwu@ee.cuhk.edu.hk).

G. Macchiarella is with the Dipartimento di Elettronica, Informazione e Bioingegneria, Politecnico di Milano, 20133 Milan, Italy (e-mail: giuseppe.macchiarella@polimi.it).

Color versions of one or more of the figures in this paper are available online at <http://ieeexplore.ieee.org>.

Digital Object Identifier 10.1109/TMTT.2016.2616866

Research efforts have been continuously devoted to synthesizing a filter matched to frequency variant complex loads. Early works on the direct synthesis with a complex load [8]–[10] date back to the 1970s, and the research has been continued by others [11]–[13]. However, these prior works mainly focus on the synthesis of channel filters in a multiplexer system. In this case, the synthesis problem is simplified, because the filter is only loaded with a frequency variant complex load at one port while still a real constant load at the other port. The synthesis for filters shown in Fig. 1 and in other advanced filtering networks though, is more challenging as the matching conditions are imposed at both the ports with both loads being frequency-dependent complex ones. An attempt was made in [14] to synthesize the channel filter in Fig. 1 based on an eigendecomposition method. Unfortunately, the approach does not provide a topology control of the filter and, therefore, is rarely used in practice. A revised analytical synthesis approach with reinforced topology control is also proposed in [14]. However, it is only applicable to a simple junction model and still relies on numerical optimization to obtain an asymmetric filtering response. Moreover, the approach is only applicable to the parallel-connected dual band filtering network. A more general synthesis of complex loaded filter is proposed in [15] by assuming the complex loads are frequency-independent constants. In a practical complex filtering network though, the complex loads are always frequency dependent, which violates the assumption.

In this paper, a general direct synthesis approach to the design of a Chebyshev bandpass filter with its two ports being matched to complex frequency variant loads is proposed. This approach greatly simplifies the design of filters in an advanced microwave network. The proposed approach is based on the power wave renormalization theory [16] and two legitimate assumptions: 1) the prescribed transmission zeros are stationary and 2) the reflection zeros are located along the imaginary axis of the complex frequency plane. Three simultaneous synthesis equations are derived from the renormalization theory and for the first time they are sequentially applied to ensure the filter is always physically realizable while optimally maintaining good matching with the complex loads. Unlike the method presented in [17], where the approach is only applicable to some simple junctions, the approach in this paper is now incorporated with an adjusting process of junction parameters to enable designs employing a general junction network. The inclusion of the adjustment process is very important, as the original synthesis approach has no mechanism to improve the complex load impedances faced by the filters.

In this paper, the load impedance is defined by the complex impedance over the band of physical frequency f . The impedance is then mapped to the low-pass prototype domain through the frequency transformation $\omega = f_0/BW (f/f_0 - f_0/f)$, where BW and f_0 denote the bandwidth and the center frequency of the filter being synthesized. In addition, the variable s refers to the complex frequency variable in the low-pass prototype domain where the coupling matrix is defined. By iteratively synthesizing each filter using the proposed synthesis approach, with an adjustment

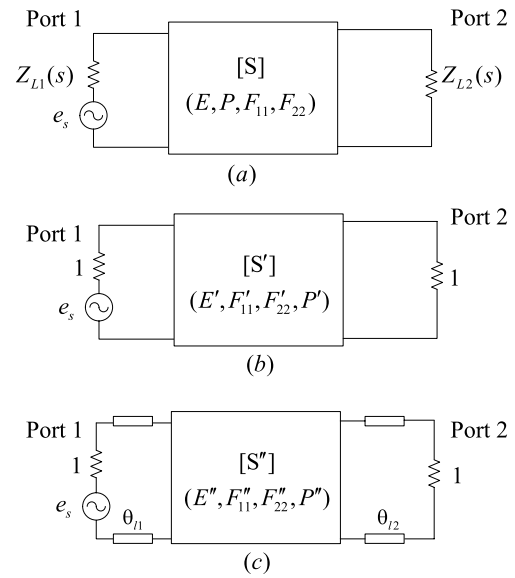


Fig. 2. Same filter network reference to different load terminations and an approximation with a coupled resonator network and two pieces of transmission line. (a) Filter network matches the frequency complex loads $Z_{L1}(s)$ and $Z_{L2}(s)$, having a scattering response $[S]$. (b) Same filter network as in (a) but referenced to unity loads at both ports, having a scattering response $[S']$. (c) Realizable filter network that optimally approximates the filter network in (b).

process of the junction parameters applied after each iteration, a complicated microwave filtering network can be designed efficiently. Details of the direct synthesis theory and a junction adjustment process for synthesizing an advanced filtering network will be described in the following section. Three synthesis examples will be provided to demonstrate the effectiveness of the proposed design procedure. Finally, a conclusion is made at the end.

II. THEORY

A. Direct Synthesis Approach

Consider the circuit shown in Fig. 2(a), where a matched filter is terminated by a general frequency variant load $Z_{L1}(s)$ at its port 1 and $Z_{L2}(s)$ at port 2. Denote the matched scattering matrix as $[S]$. Fig. 2(b) shows the same filtering circuit but with both the terminations set to unity, which complies with the definition of a filter network in a measurement state, in which both the ports are terminated by a constant real load. The measurable response is denoted as $[S']$. Based on the power wave renormalization theory, the resultant scattering matrix $[S']$ is related to $[S]$ through (1), where $r_i = (1 - Z_{Li})/[1 + (Z_{Li})^*]$, $i = 1$ or 2 , $\Delta_S = [(1 - r_1 S_{11})(1 - r_2 S_{22})] - r_1 r_2 S_{12} S_{21}$ and $*$ denotes the complex conjugate

$$S'_{11} = \left[\frac{S_{21} r_2 S_{12} + (S_{11} - r_1^*)(1 - r_2 S_{22})}{(1 - r_1^*) \Delta_S} \right] (1 - r_1) \quad (1a)$$

$$S'_{22} = \left[\frac{S_{21} r_1 S_{12} + (S_{22} - r_2^*)(1 - r_1 S_{11})}{(1 - r_2^*) \Delta_S} \right] (1 - r_2) \quad (1b)$$

$$S'_{21} = \frac{\sqrt{\text{Re}(Z_{L2})}}{\sqrt{\text{Re}(Z_{L1})}} (1 - r_1) \left[\frac{S_{21} (1 - r_2 S_{22}) + (S_{22} - r_2^*) r_2 S_{21}}{(1 - r_2^*) \Delta_S} \right]. \quad (1c)$$

Two sets of characteristic polynomials are defined here: one describes the objective matched scattering matrix [S] with

$$S_{11} = \frac{F(s)}{E(s)} \quad S_{21} = \frac{P(s)}{\varepsilon E(s)} \quad S_{22} = \frac{F_{22}(s)}{E(s)} \quad (2a)$$

and the other describes the measurable responses

$$S'_{11} = \frac{F'(s)}{E'(s)} \quad S'_{21} = \frac{P'(s)}{\varepsilon' E'(s)} \quad S'_{22} = \frac{F'_{22}(s)}{E'(s)}. \quad (2b)$$

The relation between [S] and [S'] in terms of characteristic polynomials is derived by substituting (2) into (1) and simplifying the expressions by making use of the equation $P(s)^* = (-1)^N [-P(s)]$ and the power conservation equation $(-1)^N F(s) \cdot F(s)^* - P(s) \cdot P(s)^* / \varepsilon^2 = (-1)^N E(s) \cdot E(s)^*$, with N being the filter order. The result is given in (3), as shown at the bottom of this page. $F'_{22}(s)$ is not shown because the unitary condition stipulates $F'_{22}(s) = (-1)^N [F'_{11}(s)]^*$. There are three conditions that should be simultaneously enforced in (3). The first condition requires the polynomials on the left to represent a matched response, but they do not need to be realized by a coupled resonator network. The second condition demands the measurable polynomials on the right to be always physically realizable by a coupled resonator network. Last but not least, the power conservation law should always be strictly valid to both the sets of polynomials. To meet all the three conditions, a synthesis approach is proposed based on (3) to approximate the measurable polynomials with a pure coupled resonator network and two pieces of transmission line, one on each port. Using the proposed synthesis approach, it turns out that the circuit shown in Fig. 2(c) represents a very good approximation of the measurable response and optimally satisfies (3) over the frequency band of interest. The details of the synthesis procedure are given below.

Step 1: Stipulating the measurable polynomial $P'(s)$ with its prescribed transmission zeros p'_i by

$$P'(s) = \frac{1}{\varepsilon'} e^{j\theta_p} \prod_i^{nfz} (s - p'_i) \quad (4)$$

where nfz denotes the number of transmission zeros, and ε' and θ_p are two unknown constants temporarily set to 1 and 0, respectively. Their values will be updated later.

Step 2: Determining the matched polynomial $P(s)$ by (3a), using a least square fitting over the band of interest. To minimize the error, the fitting order of $P(s)$ is set to $(N - 1)$. Note $P(s)$ in general does not satisfy the requirement of a physically realizable filter, as its roots in general will not be symmetric about the imaginary axis.

Step 3: Synthesizing the matched polynomials $F_{22}(s)$, $E(s)$ and the normalization constant ε with the roots of $P(s)$, prescribed return loss and filter order N , under the assumption that the matched response [S] satisfies a general Chebyshev function, by which the reflection zeros are purely imaginary. Update ε' by $\varepsilon' = \varepsilon$.

Step 4: Determining $F'(s)$ by (3b) through a least square fitting of an N th order polynomial over the band of interest. Denote its highest coefficient as $f'_N = |f'_N| e^{j\theta_{fN}}$ to account for a complex value. The unitary relation stipulates $F'_{22}(s) = (-1)^N [F'(s)]^*$ so it is not necessary to fit $F'_{22}(s)$ separately.

Step 5: Solving the roots of $E'(s)$ using the Hurwitz criterion and the magnitude of its highest coefficient e'_N through the power conservation relation among $P'(s)$, $F'(s)$ and $E'(s)$

$$E'(s)E'(s)^* = F'(s)F'(s)^* + P'(s)P'(s)^* / \varepsilon'^2. \quad (5)$$

Obviously $|e'_N| = |f'_N|$ since $P'(s)$ has a lower order than N for most practical applications. The phase for e'_N , i.e., θ_e , is then optimally set to a constant value to minimize the phase difference with respect to (3c).

Step 6: Specifying a set of new polynomials $E''(s)$, $P''(s)$, and $F'_{11}(s)$ that relate with $E'(s)$, $P'(s)$, and $F'(s)$ through

$$F'(s) = \sum_{i=0}^N f'_i s^i = f'_N \sum_{i=0}^N (f'_i / f'_N) s^i = |f'_N| e^{j\theta_{fN}} F'_{11}(s) \quad (6a)$$

$$E'(s) \approx |f'_N| e^{j\theta_e} \prod_{i=1}^N (s - s_i) = |f'_N| e^{j\theta_e} E''(s) \quad (6b)$$

$$P'(s) = e^{j\theta_{p'}} P''(s) \quad (6c)$$

where f'_i refers to the i th coefficients of $F'(s)$ and s_i denotes the i th roots of $E'(s)$. Equation (6) suggests that both polynomials $E''(s)$ and $F'_{11}(s)$ are monic polynomials. In addition, the polynomial $P''(s)$ is the same as $P'(s)$, except for a constant phase shift $\theta_{p'}$. If the value of θ_p in (4) is selected to be identical to that of $\theta_{p'}$ and is realized by a piece of transmission line, then $E''(s)$, $P''(s)$, and $F'_{11}(s)$ comply with a coupled resonator filter network. Substituting (6) into (2b) with the unitary relation results as

$$S'_{11}(s) = \frac{F'(s)}{E'(s)} = \frac{|f'_N| e^{j\theta_{fN}} F'_{11}(s)}{|f'_N| e^{j\theta_e} E''(s)} = e^{-j2\theta_{11}} \frac{F'_{11}(s)}{E''(s)} \quad (7a)$$

$$S'_{22}(s) = \frac{F'_{22}(s)}{E'(s)} = \frac{|f'_N| e^{-j\theta_{fN}} [F''(s)]^*}{|f'_N| e^{j\theta_e} E''(s)} = e^{-j2\theta_{22}} \frac{[F'_{11}(s)]^*}{E''(s)} \quad (7b)$$

$$S'_{21}(s) = \frac{P'(s)}{\varepsilon' E'(s)} = \frac{e^{j\theta_{p'}} P''(s)}{\varepsilon' |f'_N| e^{j\theta_e} E''(s)} = e^{-j(\theta_{11} + \theta_{22})} \frac{P''(s)}{E''(s)}. \quad (7c)$$

$$P'(s) = 4\sqrt{\text{Re}[Z_{L1}(s)]}\sqrt{\text{Re}[Z_{L2}(s)]}P(s) \quad (3a)$$

$$F'(s) = [1 + Z_{L1}(s)](-1)^N \{ [1 + Z_{L2}^*(s)]F_{22}^*(s) - [1 + Z_{L2}(s)]E^*(s) \} \\ - [1 - Z_{L1}^*(s)] \{ [1 + Z_{L2}^*(s)]E(s) - [1 - Z_{L2}(s)]F_{22}(s) \} \quad (3b)$$

$$E'(s) = [1 + Z_{L1}^*(s)] \{ [1 + Z_{L2}^*(s)]E(s) - [1 - Z_{L2}(s)]F_{22}(s) \} \\ - [1 - Z_{L1}(s)](-1)^N \{ [1 + Z_{L2}^*(s)]F_{22}^*(s) - [1 - Z_{L2}(s)]E^*(s) \} \quad (3c)$$

Equation (7) reveals that the measurable $[S']$ can be well approximated by a pure coupled resonator network $[S'']$ with a transmission line inserted between each port and its complex load. The transmission line lengths are determined by $\theta_{l1} = (\theta_e - \theta_{f11N})/2$, $\theta_{l2} = (\theta_e + \theta_{f11N})/2$. Finally, the value of θ_p in (4) is updated by $\theta_p = \theta_e - (\theta_{l1} + \theta_{l2})$.

B. Application to Complex Filtering Networks

Given the complex loads, the proposed synthesis approach optimally approximates the measurable response by minimizing the phase difference between the $E'(s)$ in (3c) and that in (6b) using a constant phase θ_e , which is then extracted out as a section of transmission line with an electrical length θ_{l1} or θ_{l2} . To account for the dispersion, θ_{l1} and θ_{l2} are converted into physical dimensions by evaluating them at the center frequency assuming the dispersion is known.

However, if the load impedance, either $Z_{L1}(s)$ or $Z_{L2}(s)$, changes significantly over the frequency band of interest, the approximation error of the measurable response will be quite large because the phase variation in (3c) may not be a smooth function. In other words, it is not guaranteed that the proposed synthesis approach can match a filter with any frequency variant complex load. In practice, when designing a filtering network that consists of multiple complex loaded filters, the synthesis approach can be iteratively applied to each channel filter. Each time the synthesis not only produces a network that optimally matches the complex loads, but also effectively adjusts the complex loads seen by filters other than the one being synthesized. As the number of iterations increases, both the load impedance $Z_{L1}(s)$ and $Z_{L2}(s)$ will gradually become smooth. The synthesized coupling matrix and the transmission line length for each filter eventually get converged. Yet, it is possible that the converged result still fails to meet the specifications as the load impedance is also affected by the junction parameters, which are not fully adjustable by application of the synthesis approach. For example, in a waveguide multiplexer design, both the stub lengths and the spacing are very critical to a waveguide multiplexer design. Given a set of improper spacing, it is possible that a channel filter can never be matched with the loads even if an optimization is applied.

To provide an additional control of the junction property, an adjustment of the junction parameters is introduced after the iterative synthesis converged. Fig. 3 shows the flowchart of the generalized design procedure for an advanced filtering network. Assuming after the convergence is achieved, the first derivatives $d[Z_{L1}(s)]/ds$ and $d[Z_{L2}(s)]/ds$ for each filter remain as small as possible within its passband, the objective of the adjustment in Fig. 3 is to minimize the derivatives. Ideally, if both Z_{L1} and Z_{L2} in (3) are complex constants, a set of suitable polynomial solutions are guaranteed. As the adjustment is only applied to a few parameters of the junction, it is much simpler than the traditional optimization design methods [5], [6].

III. SYNTHESIS EXAMPLES

A. Design of Parallel-Connected Dual Band Filter

A parallel-connected dual band filter with an asymmetric response is designed to verify the proposed synthesis method.

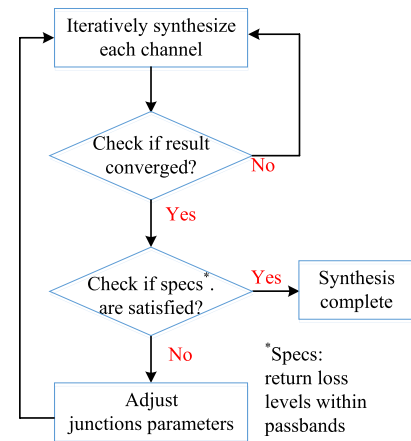


Fig. 3. Proposed design procedure for an advanced filtering network.

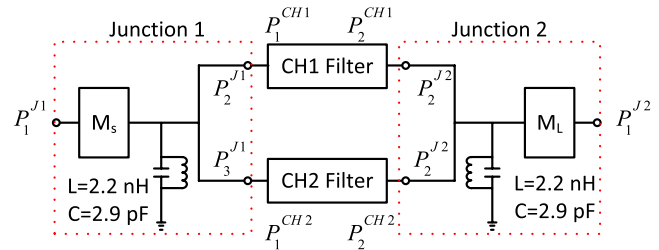


Fig. 4. Interconnections of the parallel dual band filter and initial junction models.

The center frequency of the dual band filter is 1.96 GHz and the bandwidth is 0.145 GHz. The connectivity of the filter network, including the junction models, is shown in Fig. 4. It is assumed that all the ports, including the junction ports, are referenced to 50Ω . The I/O couplings M_s and M_L are randomly set to 0.6397 and 0.7706, respectively. The center frequencies for the eighth-order CH1 filter and the fourth order CH2 filter are 1.9 and 2.02 GHz, respectively. The bandwidth for CH1 is 31 MHz while that for CH2 is 19 MHz. Three transmission zeros are prescribed for CH1, which are located at 1.88, 1.92, and 1.925 GHz. The required equiripple return loss for both the channels is 23 dB. Initially, both the channel filters are synthesized as Chebyshev doubly terminated filters using the conventional direct synthesis approach [1].

By iteratively applying the synthesis routine to each channel filter, the response is quickly converged after three iterations. The intermediate coupling matrices (in folded form) and the transmission line lengths after each iteration are summarized in Table I, while the scattering response at each step is shown in Fig. 5. It can be observed that the differences in the coupling values and the scattering response between the second and third iterations are sufficiently small. Therefore, the convergence is justified. It is also interesting to note that the synthesized S_{21} has an extra transmission zero around 1.94 GHz. This transmission zero is actually attributed by the loading effects in (3a). To facilitate the physical implementation, the folded matrix of CH1 after the third iteration is reconfigured into a trisection topology by following the

TABLE I
COUPLING MATRICES AND TRANSMISSION LINE LENGTH FOR EACH ITERATION

CH1				
	0 th	1 st	2 nd	3 rd
M ₀₁	1.0439	0.7808	0.7797	0.7811
M ₁₂	0.8641	0.8374	0.8380	0.8393
M ₂₃	0.6007	0.5992	0.6026	0.6013
M ₃₄	0.5307	0.5298	0.5330	0.5319
M ₄₅	0.5996	0.5995	0.5918	0.5947
M ₅₆	0.4728	0.4722	0.4716	0.4716
M ₆₇	0.5963	0.5937	0.6001	0.5974
M ₇₈	0.8641	0.8263	0.8297	0.8307
M _{8L}	1.0439	0.6406	0.6411	0.6418
M ₁₁	0.0045	0.0363	-0.0269	-0.0116
M ₂₂	0.0049	0.0066	-0.0029	0.0008
M ₃₃	0.0057	0.0069	-0.0034	0.0003
M ₄₄	0.1365	0.1356	0.1325	0.1337
M ₅₅	-0.4965	-0.4897	-0.5246	-0.5123
M ₆₆	-0.0290	-0.0261	-0.0443	-0.0373
M ₇₇	0.0049	0.0086	-0.0095	-0.0025
M ₈₈	0.0045	0.0483	-0.0716	-0.0462
M ₃₆	-0.1431	-0.1422	-0.1406	-0.1413
M ₃₇	-0.0725	-0.0712	-0.0746	-0.0733
M ₄₆	0.3140	0.3102	0.3263	0.3206
θ_1 (rad)	NA	-0.0031	0.0164	0.0087
θ_2 (rad)	NA	-0.0037	0.0253	0.0147
CH2				
	0 th	1 st	2 nd	3 rd
M ₀₁	1.1055	0.8349	0.8351	0.8356
M ₁₂	0.9860	0.9656	0.9657	0.9660
M ₂₃	0.7411	0.7401	0.7407	0.7412
M ₃₄	0.9860	0.9609	0.9615	0.9621
M ₄₅	1.1055	0.6907	0.6936	0.6955
M ₁₁	0.000	0.0013	0.0392	0.0595
M ₂₂	0.000	0.0034	0.0073	0.0092
M ₃₃	0.000	0.0049	0.0095	0.0117
M ₄₄	0.000	0.0705	0.1343	0.1649
θ_1 (rad)	NA	0.0007	0.0008	0.0009
θ_2 (rad)	NA	-0.0033	-0.0057	-0.0065

sequence of matrix rotation suggested in [1]. The transmission lines are then transformed to equivalent nonresonant nodes connected in parallel with the common resonators in Fig. 4 using the extracted pole method [18]. Based on the synthesized circuit model, a coaxial filter is designed and fabricated. Fig. 6 shows a photograph of the fabricated filter highlighted in a dashed box, which is one of four dual band filters in an integrated filter module. The measurement result is shown in Fig. 7, superposed with the synthesis result. Due to the fabrication tolerance and the dispersion effect of the resonant junctions at both the ports, the measured response

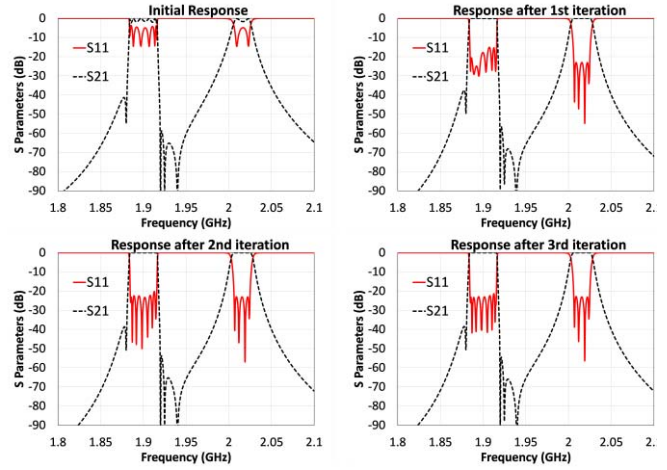


Fig. 5. Responses for each iteration of the dual band filter design.

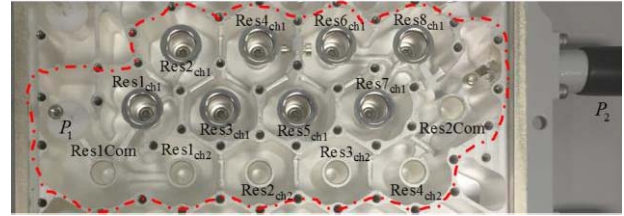


Fig. 6. Photograph of the fabricated dual band filter.

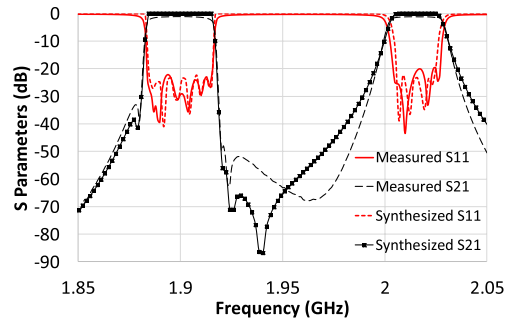


Fig. 7. Measured and synthesized scattering responses of the dual band filter.

of CH2 slightly deviates from the synthesized one in the interband rejection. This design example has demonstrated the effectiveness of the proposed synthesis approach.

B. Masthead Combiner

A masthead combiner is a microwave device designed to improve the signal-to-noise ratio of a transceiver system when the antenna is mounted on top of a mast [4]. Fig. 8 shows a block diagram of a masthead combiner. It is composed of three filters and an LNA connected through a pair of junctions. Assuming the LNA design is referenced to 50Ω at both the ports, then for filters Rx1 and Rx2 the load seen toward the junction is a frequency variant complex value. For the filter Tx, both the ports are required to match the frequency variant complex loads. Different from the design approach reported in [4], where an optimization is applied to seek for a solution, now an analytical design is obtained by applying the

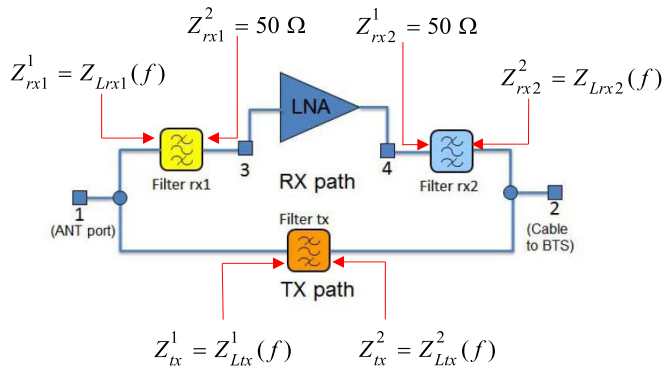


Fig. 8. Block diagram of a masthead combiner [4].

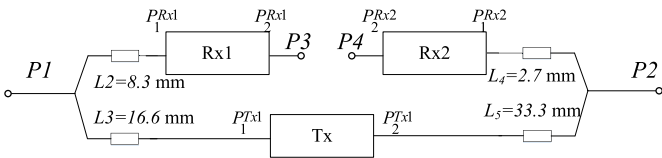


Fig. 9. Interconnections of the masthead combiners and initial junction models.

TABLE II
SPECIFICATIONS OF THE MASTHEAD COMBINER

	Rx1	Rx2	Tx
Filter order	7	7	9
Return loss(dB)	20	20	20
Transmission zeros (MHz)	883,892,902	NA	909
Center frequency f_0 (MHz)	850	850	950
Bandwidth BW (MHz)	55	55	55

proposed synthesis routine iteratively to all the three filters. The specifications for each filter are summarized in Table II. In addition, the initial junctions and the interconnections are shown in Fig. 9. For simplicity, it is assumed that all the transmission lines are ideal and have a characteristic impedance of 50Ω . The junction is simulated using a circuit simulator. Due to the simplicity of the junction model, the adjustment of junction parameters shown in Fig. 3 is not necessary. The synthesis quickly gets converged after five iterations, and the simulated scattering response is shown in Fig. 10. As can be seen, all the specifications are satisfied and the return loss within the passbands is almost equiripple. Finally, the coupling routine of the equivalent nonresonant node circuit is shown in Fig. 11, where the nonresonant nodes are labeled by the gray circles and the resonator nodes are denoted by the black circles.

C. Waveguide Dual Multiplexer

A waveguide dual multiplexer network directly connects a splitting multiplexer and a combing multiplexer through one of the channel filters [5]. Fig. 12 shows a block diagram of a dual multiplexer system. All the channel filters can be synthesized by the proposed routine. For illustration, a dual multiplexer similar to that shown in Fig. 12 is designed. The specifications

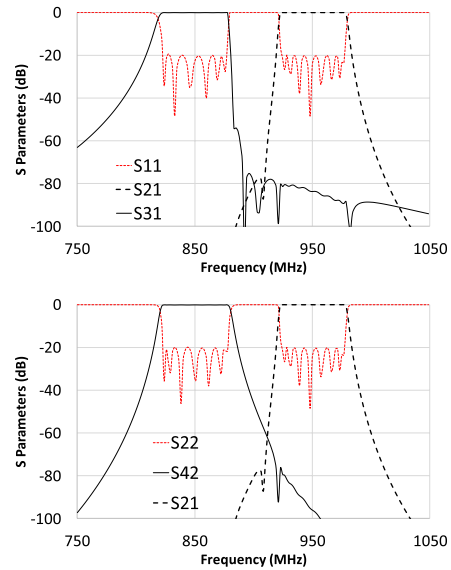


Fig. 10. Scattering response of the synthesized masthead combiner.

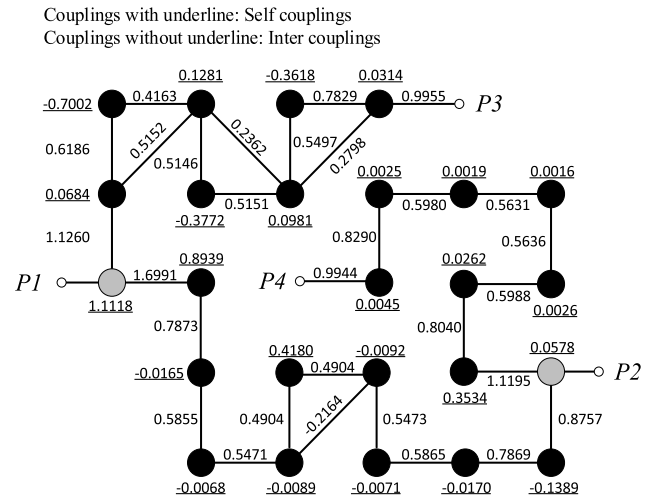


Fig. 11. Coupling routines of the masthead combiner.

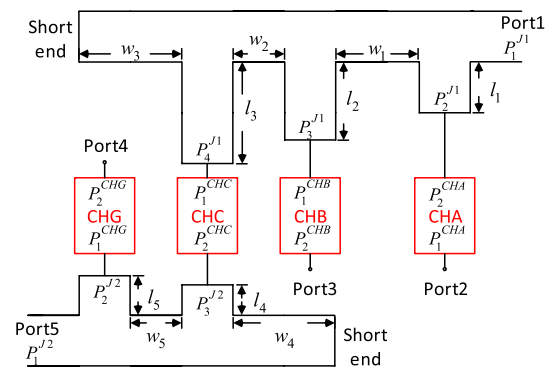


Fig. 12. Block diagram of a dual multiplexer system.

for each channel filter are listed in Table III. The initial dimensions of the WR-51 waveguide manifolds in Fig. 12 are determined by following the design guideline given in [19] as follows: $l_1 = 1.142$, $l_2 = 1.22$, $l_3 = 1.43$, $l_4 = 1.167$, $l_5 = 1.05$, $w_1 = 1.891$, $w_2 = 1.812$, $w_3 = 0.659$, $w_4 = 0.781$,

TABLE III
SPECIFICATIONS OF THE DUAL MULTIPLEXER

	CHA	CHB	CHC	CHG
Filter order	5	5	4	6
Return loss(dB)	25	25	25	25
Transmission zeros (GHz)	17.84, 17.89	18.93, 19.18	17.82 18.04	NA
Center frequency f_0 (GHz)	17.76	19.07	17.93	18.5
Bandwidth BW (MHz)	112.5	150	75	585

TABLE IV
FINAL DIMENSION OF THE MANIFOLD JUNCTIONS (INCHES)

l_1	0.228	w_1	0.169
l_2	2.435	w_2	0.474
l_3	1.289	w_3	0.659
l_4	1.328	w_4	0.258
l_5	1.336	w_5	0.439

TABLE V
SYNTHESIZED COUPLING MATRIX FOR EACH CHANNEL FILTER

CHA		CHB		CHC		CHG	
M_{S1}^{CHA}	1.2780	M_{S1}^{CHB}	0.7244	M_{S1}^{CHC}	0.9552	M_{S1}^{CHG}	0.7120
M_{12}^{CHA}	0.8661	M_{12}^{CHB}	0.6810	M_{12}^{CHC}	0.9456	M_{12}^{CHG}	0.8370
M_{23}^{CHA}	0.6604	M_{23}^{CHB}	0.5865	M_{23}^{CHC}	0.7905	M_{23}^{CHG}	0.6441
M_{34}^{CHA}	0.6507	M_{34}^{CHB}	0.7452	M_{34}^{CHC}	0.9455	M_{34}^{CHG}	0.6120
M_{45}^{CHA}	0.9739	M_{45}^{CHB}	0.8979	M_{45}^{CHC}	0.4406	M_{45}^{CHG}	0.6468
M_{S1}^{CHA}	1.1206	M_{S1}^{CHB}	1.0835	M_{S1}^{CHC}	-0.0863	M_{S1}^{CHG}	0.9374
M_{24}^{CHA}	0.1742	M_{24}^{CHB}	0.1187	M_{24}^{CHC}	-0.2485	M_{24}^{CHG}	1.1014
M_{25}^{CHA}	0.0164	M_{25}^{CHB}	-0.1834	M_{25}^{CHC}	0.0181	M_{25}^{CHG}	-0.4900
M_{11}^{CHA}	1.0728	M_{11}^{CHB}	-0.2972	M_{11}^{CHC}	0.0016	M_{11}^{CHG}	-0.0956
M_{22}^{CHA}	0.0339	M_{22}^{CHB}	0.0014	M_{22}^{CHC}	0.3327	M_{22}^{CHG}	-0.0060
M_{33}^{CHA}	-0.2847	M_{33}^{CHB}	-0.1817			M_{33}^{CHG}	0.0062
M_{44}^{CHA}	0.0230	M_{44}^{CHB}	0.0679			M_{44}^{CHG}	0.0083
M_{55}^{CHA}	0.0204	M_{55}^{CHB}	0.0137			M_{55}^{CHG}	0.0105

$w_5 = 0.75$ (in inches). In this example, the adjustment in Fig. 3 is required since the spacing (w_i) requires updates if its value is improper. At the end of the synthesis routine in Fig. 3, all the coupling matrices and stub lengths converge to constant values; the adjustment is then solely applied to the spacing to minimize the variation in the complex loads to each filter at its center frequency. Unlike previous examples where the junction is simulated through a circuit simulator, the manifold junctions in this example are simulated using a mode matching program to truly reflect their electromagnetic properties. The scattering response of the dual multiplexer at the end of the proposed design procedure is shown in Fig. 13, while the final dimensions and the coupling matrices are summarized in Tables IV and V, respectively. As can be seen from Fig. 13(a), despite a slight deviation in the high passband, the return loss level is well below 22 dB within all the passbands. The insertion loss in Fig. 13(b) reveals all the transmission zeros located at the prescribed frequencies except for the lowest channel, whose transmission zeros are not explicitly shown, as the insertion loss near the zeros is below 140 dB. Nevertheless, this design demonstrates the

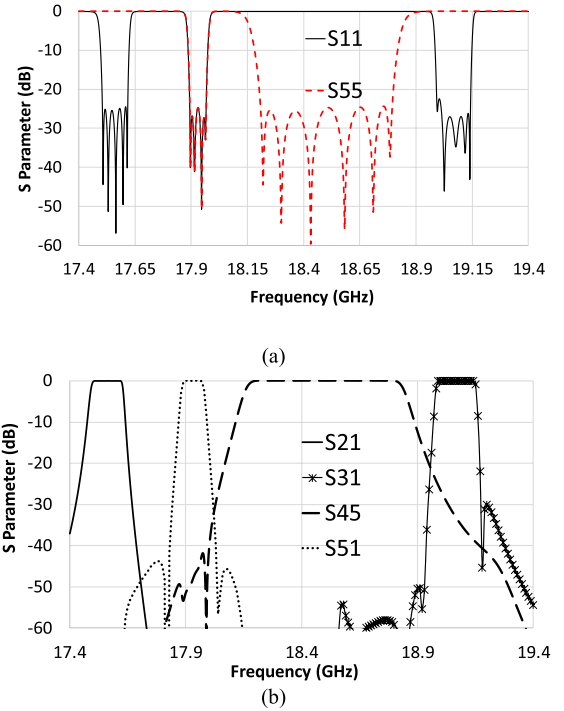


Fig. 13. Scattering response of the synthesized dual multiplexer. (a) Return loss at common ports. (b) Insertion loss of each channel.

robustness of the proposed synthesis procedure in designing a complex filtering network.

IV. CONCLUSION

A direct synthesis approach is proposed for the synthesis of a filter matched to the frequency variant complex loads at both the ports. Three equations relating the matched polynomials and the measurable polynomial are derived from the power wave renormalization theory. For the first time, these equations are directly applied to simultaneously enforce the matchability and the realizability of a filter circuit. It has been shown that a coupled resonator network cascaded with a transmission line at each port can always optimally approximate the desired filtering response in a complex filtering network. A synthesis routine is given and a general design procedure is developed by incorporating the synthesis routine with an adjustment of the junction parameters. Compared with the traditional optimization design method, the proposed design procedure is direct and requires much less variables to adjust and, therefore, is much faster and more robust. Finally, three practical design examples are provided to demonstrate the effectiveness of the proposed procedure.

REFERENCES

- [1] R. J. Cameron, "General coupling matrix synthesis methods for Chebyshev filtering functions," *IEEE Trans. Microw. Theory Techn.*, vol. 47, no. 4, pp. 433–442, Apr. 1999.
- [2] G. Macchiarella and S. Tamiazzo, "Synthesis of dual-band filters with parallel-connected networks," in *Proc. Eur. Microw. Conf. (EuMC)*, Oct. 2014, pp. 608–611.
- [3] R. Levy, R. V. Snyder, and G. Matthaei, "Design of microwave filters," *IEEE Trans. Microw. Theory Techn.*, vol. 50, no. 3, pp. 783–793, Mar. 2002.

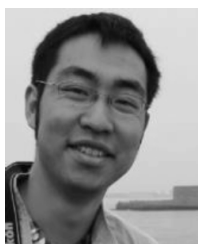
- [4] G. Macchiarella and S. Tamiazzo, "Design of 'masthead' combiners," in *Proc. Eur. Microw. Conf. (EuMC)*, Sep. 2015, pp. 686–689.
- [5] Q. Shi and M. Yu, "Ka-band dual multiplexer with a connected channel," in *IEEE MTT-S Int. Microw. Symp. Dig.*, Jun. 2013, pp. 1–3.
- [6] M. Yu and Y. Wang, "Synthesis and beyond," *IEEE Microw. Mag.*, vol. 12, no. 6, pp. 62–76, Oct. 2011.
- [7] A. Morini and T. Rozzi, "Constraints to the optimum performance and bandwidth limitations of diplexers employing symmetric three-port junctions," *IEEE Trans. Microw. Theory Techn.*, vol. 44, no. 2, pp. 242–248, Feb. 1996.
- [8] J. L. Haine and J. D. Rhodes, "Direct design formulas for asymmetric bandpass channel diplexers," *IEEE Trans. Microw. Theory Techn.*, vol. 25, no. 10, pp. 807–813, Oct. 1977.
- [9] J. Rhodes and R. Levy, "A generalized multiplexer theory," *IEEE Trans. Microw. Theory Techn.*, vol. 27, no. 2, pp. 99–111, Feb. 1979.
- [10] J. D. Rhodes and R. Levy, "Design of general manifold multiplexers," *IEEE Trans. Microw. Theory Techn.*, vol. 27, no. 2, pp. 111–123, Feb. 1979.
- [11] R. Levy, "Synthesis of non-contiguous diplexers using broadband matching theory," in *IEEE MTT-S Int. Microw. Symp. Dig.*, Boston, MA, USA, Jul. 1991, pp. 543–546.
- [12] K. L. Wu and W. Meng, "A direct synthesis approach for microwave filters with a complex load and its application to direct diplexer design," *IEEE Trans. Microw. Theory Techn.*, vol. 55, no. 5, pp. 1010–1017, May 2007.
- [13] H. Meng and K.-L. Wu, "Direct optimal synthesis of a microwave bandpass filter with general loading effect," *IEEE Trans. Microw. Theory Techn.*, vol. 61, no. 7, pp. 2566–2573, Jul. 2013.
- [14] G. Macchiarella and S. Tamiazzo, "Design techniques for dual-passband filters," *IEEE Trans. Microw. Theory Techn.*, vol. 53, no. 11, pp. 3265–3271, Nov. 2005.
- [15] C. Ge, X.-W. Zhu, X. Jiang, and X.-J. Xu, "A general synthesis approach of coupling matrix with arbitrary reference impedances," *IEEE Microw. Wireless Compon. Lett.*, vol. 25, no. 6, pp. 349–351, Jun. 2015.
- [16] K. Kurokawa, "Power waves and the scattering matrix," *IEEE Trans. Microw. Theory Techn.*, vol. MTT-13, no. 2, pp. 194–202, Mar. 1965.
- [17] H. Meng and K.-L. Wu, "Direct optimal synthesis of microwave dual band filters with parallel-connected topology," in *IEEE MTT-S Int. Microw. Symp. Dig.*, May 2016, pp. 1–4.
- [18] P. Zhao and K. L. Wu, "An iterative and analytical approach to optimal synthesis of a multiplexer with a star-junction," *IEEE Trans. Microw. Theory Techn.*, vol. 62, no. 12, pp. 3362–3369, Dec. 2014.
- [19] R. I. Cameron and M. Yu, "Design of manifold-coupled multiplexers," *IEEE Microw. Mag.*, vol. 8, no. 5, pp. 46–59, Oct. 2007.



Huan Meng received the B.Eng. (Hons.) degree in electronic and information engineering from Hong Kong Polytechnic University, Hong Kong, in 2010, and the M.Phil. degree in electronic engineering from the Chinese University of Hong Kong, Hong Kong, in 2012, where he is currently pursuing the Ph.D. degree.

His current research interests include the design and synthesis of passive microwave coupled-resonator networks, including diplexers and multiplexers.

Dr. Meng was a recipient of the Asia-Pacific Microwave Conference Prize in 2012.



Ping Zhao (S'14) received the B.Sc. degree from Nanjing University, Nanjing, China, in 2012. He is currently pursuing the Ph.D. degree at the Chinese University of Hong Kong, Hong Kong.

His current research interests include synthesis and computer-aided tuning algorithms for multi-port microwave coupled-resonator networks, including diplexers, multiplexers, and coupled-resonator decoupling networks with applications in cellular base stations and satellites.

Dr. Zhao was a recipient of the Honorable Mention at the IEEE MTT-S International Microwave Symposium Student Paper Competition in 2014 and the Best Student Paper Award of the 2014 IEEE HK AP/MTT Postgraduate Conference.



Ke-Li Wu (M'90–SM'96–F'11) received the B.S. and M.Eng. degrees from the Nanjing University of Science and Technology, Nanjing, China, in 1982 and 1985, respectively, and the Ph.D. degree from Laval University, Quebec City, QC, Canada, in 1989.

From 1989 to 1993, he was a Research Engineer and a Group Manager with the Communications Research Laboratory, McMaster University, Hamilton, ON, Canada. In 1993, he joined the Corporate Research and Development Division, COM DEV International, where he was a Principal Member of Technical Staff. Since 1999, he has been with the Chinese University of Hong Kong, Hong Kong, where he is a Professor and the Director of the Radio Frequency Radiation Research Laboratory. His current research interests include partial element equivalent circuit and physics-based model order reduction for EM modeling of high speed circuits, RF and microwave passive circuits and systems, synthesis theory and the computer aided tuning of microwave filters, antennas for wireless terminals, LTCC-based multichip modules, and RF identification technologies.

Prof. Wu is a member of the IEEE MTT-8 Subcommittee (Filters and Passive Components) and also serves as a Technical Program Committee member for many prestigious international conferences including the IEEE MTT-S International Microwave Symposium. He was a recipient of the 1998 COM DEV Achievement Award and the Asia-Pacific Microwave Conference Prize in 2008 and 2012, respectively. He was an Associate Editor of the IEEE TRANSACTIONS ON MICROWAVE THEORY AND TECHNIQUES from 2006 to 2009.



Giuseppe Macchiarella (M'95–SM'06–F'15) is currently an Associate Professor of microwave engineering with the Department of Electronic and Information, Polytechnic University of Milan, Milan, Italy. He has been a Scientific Coordinator with PoliEri, a research laboratory concentrating on monolithic microwave integrated circuits, which was jointly supported by the Polytechnic University of Milan and Ericsson. He has been responsible for several contracts and collaborations with various companies operating in the microwave industry. He

has authored or co-authored over 150 papers on journals and conferences proceedings. His research interests included the area of microwave engineering such as microwave acoustics (SAW devices), radio wave propagation, numerical methods for electromagnetic, power amplifiers, linearization techniques, and passive devices. His current research interests include the development of new techniques for the synthesis of microwave filters and multiplexers.

Dr. Macchiarella is the Vice-Chair of the IEEE Technical Committee MTT-8 (Filters and Passive Components).